Condensation Rate of Water on Aqueous Droplets in the Transition Regime

GIDEON SAGEEV,* RICHARD C. FLAGAN,* JOHN H. SEINFELD,* AND STEPHEN ARNOLD†

*Department of Chemical Engineering, California Institute of Technology, Pasadena, California 91125 and †Department of Physics, Polytechnic Institute of New York, Brooklyn, New York 11201

Received June 10, 1985; accepted November 1, 1985

The rate of condensation of water on single aqueous solution drops in the transition regime is measured with an electrodynamic balance. Observed characteristic relaxation times are compared with those predicted theoretically to determine the thermal accommodation coefficient, which is found to be unity (consistent with the accepted value in the literature). Due to the large heat of vaporization of water and the experimental conditions used, the relaxation time is relatively insensitive to the water mass accommodation coefficient, although the data would support a value close to unity.

1. INTRODUCTION

There has long been a concern in aerosol science with understanding heat and mass transfer processes to single particles in the noncontinuum regime. Several theoretical treatments are available for transport to particles in the noncontinuum regime, in which flux expressions are derived that predict transport rates from the free molecule, through the so-called transition regime, to the continuum regime. The crux of these flux theories is their dependence on the Knudsen number, $Kn = \lambda/R_p$, where λ is an appropriately defined mean free path and R_p is the particle radius. In addition, the heat and mass transfer processes are characterized by the thermal and mass accommodation coefficients, α_T and β_M, respectively. The thermal accommodation coefficient α_T can be considered as the ratio of the actual heat transfer flux to that predicted if every molecule thermally accommodates at the surface of the particle. The mass accommodation, or sticking, coefficient β_M is just the fraction of molecules that strike the surface of the particle that adhere to it. The object of the present work is to measure the rate of condensation of water on single aqueous aerosol particles in the transition regime so as to evaluate, if possible, the applicability of existing transition regime flux theories as well as thermal and mass accommodation coefficients.

In the present work water condensation rates are measured on single $(NH_4)_2SO_4$ aqueous solution droplets suspended in an electrodynamic balance, or quadrupole. The medium surrounding the particles consists of an air/water vapor or N_2/water vapor mixture. Two related studies have recently been presented. Arnold *et al.* (1) described similar experiments on suspended aqueous solution droplets in which the transport processes were in the continuum regime. The present work extends the experiments into the transition regime. Richardson *et al.* (2) have reported measurements of growth rates of NaCl solution droplets in a background of water vapor. The absence of noncondensing gas molecules (i.e., O_2 and N_2) enabled the use of self-diffusion theory in analyzing mass transfer to the droplets. The presence of noncondensing gas molecules in the current system necessitates the use of binary diffusion theory, in describing the mass transport.

0021-9797/86 $3.00

In Section 2, we describe the experimental system and how particle growth rate measurements were obtained. Section 3 is devoted to a brief summary of applicable transition regime theoretical results for heat and mass transfer rates. Finally, we present in Section 4 the experimental data obtained and their interpretation in light of the theory.

2. EXPERIMENTAL SYSTEM

2.1. The Electrodynamic Balance

The experiments described here were carried out in an electrodynamic balance. As shown in Fig. 1, the balance consists of two hyperboloidal endcap electrodes between which a dc potential is held, and a hyperbolic torus to which an ac voltage is applied. The use of this apparatus, as well as its historical development, has been documented by Davis (3). The dynamic behavior of a charged particle in the electric field inside the chamber has been presented elsewhere (4–6), thus here it will suffice to mention that a charged particle can be stably levitated in the device by applying a dc voltage between the endcaps, V_{dc}, such that

$$qC\frac{V_{dc}}{2Z_0} = mg \qquad [1]$$

where q and m are the particle charge and mass, g is the gravitational constant, Z_0 is the distance between the center of the chamber and the endcaps (which equals 4.49 mm in our case), and C is a geometric constant for the hyperbolic geometry of Fig. 1. The value of the geometric constant has been determined theoretically by several authors (4, 5). Phillip *et al.* obtained a value of 0.80 by computing the internal field numerically. Davis *et al.* (4) evaluated C by obtaining an analytical solution to the approximated field in the chamber (by neglecting the presence of the ring electrode). The theoretical value for C calculated by Davis is 0.8768. In the theoretical studies above, the effect of the ring or the effect of holes in the ring electrode has been ignored; thus, as Davis points out, the value of the geometric constant must be determined experimentally.

As shown in Fig. 1, the electrodes (made of stainless steel) are positioned within a stainless steel container. The electrical connections to the electrodes are made through the bottom

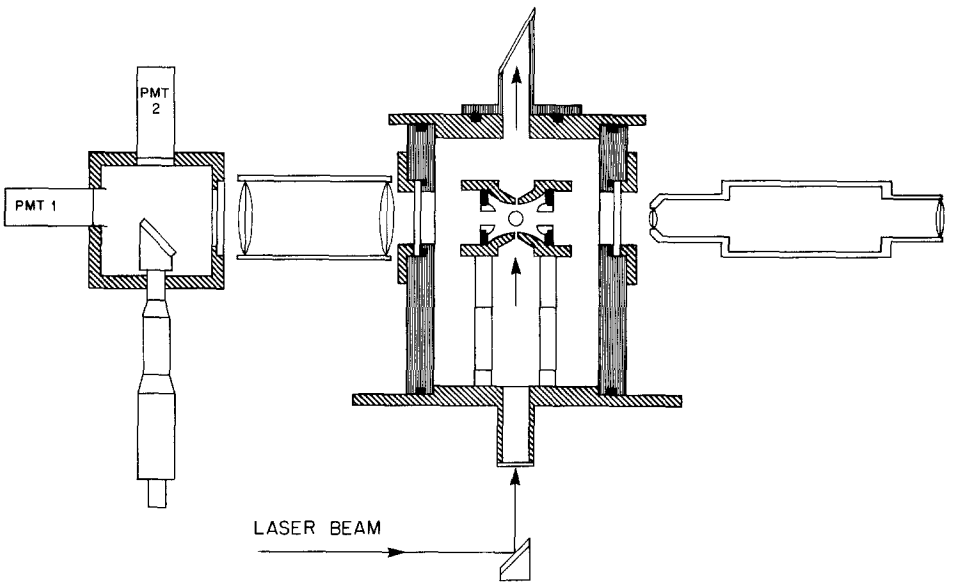

FIG. 1. A schematic diagram showing the cross section of the electrodynamic balance system.

plate, along the supporting legs of the electrodes. The particle is illuminated with a HeNe laser, the beam of which enters through the bottom window of the container and runs vertically through the chamber. The pressure in the chamber is measured with a capacitative manometer, and the temperature is monitored by a thermistor. Additionally, the chamber is held at a constant humidity through a connection to a glass bulb containing a saturated salt solution ($(NH_4)_2PO_4$ solution in the present case).

In order to facilitate the continuous monitoring of the particle balancing voltage, we have incorporated an automatic servo system into the apparatus, the basic design of which has been described by Arnold *et al.* (8). As shown in Fig. 1, the servo system functions by reimaging the particle on the edge of a 45° mirror. One photomultiplier tube is placed directly above the edge, while the other is positioned in the direction of the incident light. The optics are adjusted so that when the particle is in the center of the chamber, its image is split across the edge of the mirror. In this fashion, small vertical displacements of the particle result in different current outputs from the two photomultiplier tubes. By feeding the current output of the photomultiplier tubes into a log-ratio amplifier, a correcting signal to the balancing voltage is generated.

2.2. *Particle Insertion and Sizing*

Particles are introduced into the electrodynamic balance by first removing the topcap (including the Brewster window), and then positioning a droplet impulse jet over the top electrode. In the jet (made by Uni Photon System, Inc., Model 1), a fluid displacement is achieved by pulsing a piezoelectric crystal. The purity of the drop is ensured by first flushing the jet with purified water, and then backfilling a minute quantity of salt solution through its glass tip. The droplets are charged inductively as they leave the jet and enter the chamber.

After a particle has been trapped, the chamber is evacuated down to a pressure of about 1 Torr in order to dry out the particle and measure the balancing voltage needed to levitate the dried particle. Once this voltage is found, water vapor is bled into the chamber by opening a valve connecting the chamber to a saturated salt solution. At a particular water vapor concentration the dry particle deliquesces. The final particle size is determined by the relative humidity in the chamber which is governed by the saturated salt solution. The water content of the droplet is computed from the relative voltages of the dry and the deliquesced particle. After the droplet size has stabilized, either air or N_2 is bled slowly into the chamber, raising the pressure to a desired level.

At this point the particle size (which is needed in the subsequent rate calculations) is determined either by its sedimentation rate, or from its "spring-point" potential (6). When using the sedimentation method, the particle initial balancing voltage, V_{dc}^0, is first changed to a new value, V_{off}. The ac field is then turned off and the particle begins to move under the combined influence of gravity and the electric field. In this case a force balance on the particle yields

$$mg - \frac{qC}{2Z_0} V_{off} = \frac{6\pi R_p \mu}{C_c} v \qquad [2]$$

where R_p and v are the particle radius and terminal velocity, C_c is the Cunningham correction factor to Stokes drag, and μ is the gas viscosity. Since the particle charge to mass ratio is known from the initial balancing voltage, the radius R_p can be found by straightforward manipulation of Eq. [2], resulting in

$$R_p = \left(\frac{9\mu v}{2C_c\rho_p g}\left[\frac{V_{dc}^0}{V_{dc}^0 - V_{off}}\right]\right)^{1/2}. \qquad [3]$$

It should be pointed out that when using this method, the particle was only allowed to fall about 1 mm around the center of the chamber where the field is relatively uniform. For particles under current investigation (10–20 μm in diameter), an offset of $\approx$2% from the initial voltage, resulted in fall times of 2–5 s. The falling particles were observed through a cal-

ibrated reticle of a 30× microscope, and timed manually as they passed through a given distance on the reticle. With the balancing voltage known to 0.1% and assuming that human response time is ≈100 ms, the uncertainty in the velocity measurement is ≈5%, while for a 2% offset voltage, the uncertainty in the term $[V_{dc}^0/(V_{dc}^0 - V_{off})]$ is also 5%. Thus the uncertainty in the radius evaluation at atmospheric pressure (where $C_c \approx 1$) is about 5% for a single measurement.

When using the "spring-point" method, the ac trapping voltage is increased to the point at which the particle becomes unstable and begins to oscillate at half the driving frequency (6). Instability diagrams for the hyperbolic geometry, which show the regions of stable and unstable levitation, have been presented elsewhere (4). In these diagrams, the instability envelope is expressed as a function of the drag and electric field parameters, $\bar{k}$ and Q; where $\bar{k} = (12\pi R_p \mu)/(C_c m\omega)$ (for a sphere) and $Q = (8V_{ac}^* g)/(\omega^2 Z_0 V_{dc}^0 C)$, in which V_{ac}^* is the spring-point voltage and ω is the driving frequency (60 Hz in this case). As evident from the equation above, the calculation of Q requires knowledge of the cell constant C. The value of C for our chamber was found experimentally by placing PSL particles in the chamber and measuring their size from the fall rate and the spring-point method. Since the radius obtained by the fall rate is independent of C, we used results of that method to calibrate the particle. Knowing the radius of the particle, the value of C was varied until the radii obtained by both methods were equal. Our experimental value of C is 0.71, about 10% lower than the theoretical value. This reduction is also in agreement with data presented by Phillip (7) which were obtained in an identical chamber. Thus by measuring V_{ac}^*, Q can be calculated and the radius is found from the corresponding value of the drag parameter. It should be mentioned that this sizing technique has also been used by Richardson *et al.* (2); however, in the case in which the particles are solid crystals a shape factor multiplying the Stokes drag is required.

2.3. *The Growth-Rate Measurement*

Particle growth rates were measured by the method of Arnold *et al.* (1). For completeness a short description of the method is included in what follows. Once the particle diameter is determined, the particle size is decreased slightly from its equilibrium value by heating the droplet, and the rate at which it grows back to its original size once the heating is terminated is recorded. In the first step in the growth rate measurement the automatic servo system is turned on and the microscope eyepiece (Figs. 1 and 2) is replaced with a photomultiplier tube. As is evident from Fig. 1, the photomultiplier tube is positioned so as to receive the 90° scattered light from the particle. At this point the shutter, shown in Fig. 2, is opened for $\frac{1}{2} - \frac{1}{32}$ s, thereby exposing the particle to an IR heat source (consisting of a coiled Nicrome wire). During the heating the particle evaporates slightly and the change in size is reflected by a change in the scattering signal from the photomultiplier tube. The scattering signal is recorded either on a storage scope or on an X–Y recorder from which the particle relaxation time may be determined.

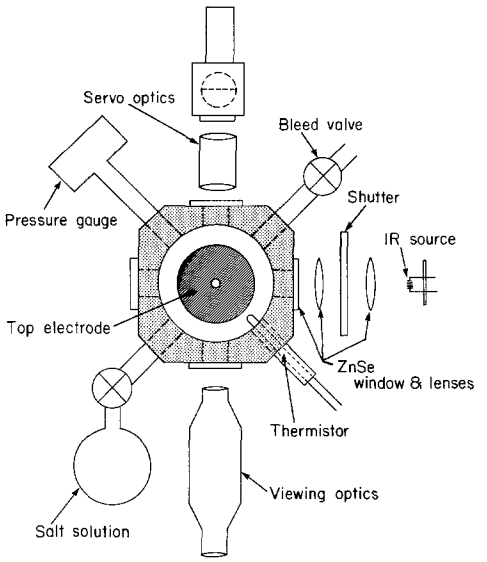

FIG. 2. A schematic diagram of the top view of the electrodynamic balance system.

The relationship between the change in the scattered light intensity S from the particle and the change in its diameter is (1, 10)

$$\frac{\Delta S}{S} = \beta \frac{\Delta R_p}{R_p} \qquad [4]$$

where β is a transfer function which can become very large ($>10^3$) near resonance. In converting the scattering signal to growth rates it is crucial that the value of β remains constant. As long as β remains constant, the size relaxation time constant is equal to the scattered light relaxation time constant; thus an exact knowledge of the value of β is not necessary. To ensure a constant β, we produce only small size fluctuations by heating the particle for a short period. Additionally, the same particle is heated for several different times to check that the relaxation rate remains constant for different changes in the radius. For each reported measurement the decay in the scattered light fluctuation, following heating, was found to be exponential, which as shown by Arnold *et al.* (1) is consistent with a constant value for β.

3. RESPONSE OF AN AQUEOUS DROP TO HEATING AND COOLING

When describing the dynamic behavior of a droplet, initially in equilibrium with its surroundings, whose temperature is suddenly perturbed, one must account for both heat and mass transfer from the drop. In an earlier work, Sageev and Seinfeld obtained both analytical and numerical solutions for the temperature and size of an evaporating drop under the influence of an intense heat source (11). Those solutions are not applicable here as we are interested in the cooling period, after the heat source is turned off. The description of this process has been addressed by several authors (1, 12–14), the most comprehensive treatment of which is that of Wagner (12). The theoretical development of Arnold *et al.* (1) can form the basis for extension of the theory of particle growth into the transition regime. We also have noted in the Introduction that another goal of the present study is to obtain estimates of the thermal accommodation coefficient, α_T, and the condensation coefficient, β_M for water. These coefficients arise in the correction terms describing the deviation of the growth rate from that in the continuum regime. As pointed out by Wagner (12), since these correction terms become more dominant as the Knudsen number Kn is increased, it is best to work in either the free molecule or transition regimes in order to obtain estimates of the α_T and β_M.

The mass flux from a drop can be expressed as

$$J_M = \varphi_M D_g \left(\frac{\partial C}{\partial r}\right)_{r=R_p} \qquad [5]$$

where C is the mass concentration of the diffusing species, D_g is the binary diffusion coefficient of the diffusing species in the background gas, and φ_M is the noncontinuum correction to the mass flux. Various forms of φ_M have appeared in the literature (3). For example, by an approximate solution to the Boltzmann equation, Sitarski and Nowakowski (15) obtained the following expression for φ_M:

$$\varphi_M = \frac{1 + 3\beta_M(1 + Z_{ij})^2 \mathrm{Kn}/4(3 + 5Z_{ij})}{1 + \dfrac{15\pi(1 + Z_{ij})^2}{4(9 + 10Z_{ij})}\left[\left(\dfrac{\beta_M(1 + 2Z_{ij})}{\pi(3 + 5Z_{ij})} + \dfrac{1}{2\beta_M}\right)\mathrm{Kn} + \dfrac{9(1 + Z_{ij})^2}{8(3 + 5Z_{ij})}\mathrm{Kn}^2\right]} \qquad [6]$$

where Z_{ij} is the ratio of the molecular weight of the diffusing species to that of the background gas. We use the equation above to describe φ_M because in an earlier work by Davis (16, 17), mass transfer data were modeled accurately using the same expression.

It should be pointed out that when there exist several vapor species in the system, the

mean free path for thermal transport λ_T differs from that for mass transport λ_M. The reason for this difference is that heat conduction is carried out by both the diffusing species and the background gas, whereas mass transfer results from the transfer of the diffusing species alone. Therefore we consider λ_T to be the average distance between collisions in the gas mixture, while λ_M is taken as the distance the diffusing species, in our case water molecules, travel between collisions. In the present work we will base the calculations of the Knudsen number on λ_T because, as will be shown in the next section, due to the large heat of vaporization of water the thermal correction φ_T dominates the growth rate of the drop. The computation of λ_T was based on the average properties of the gas mixture through the equation (18)

$$\lambda_T = \frac{\mu}{0.499\rho\bar{c}} \qquad [7]$$

where $\bar{c}$ is the average molecular velocity in the gas.

Since heat conduction through the drop is much faster than that through the gas, the Biot number for the drop/gas system is much less than unity. Under these circumstances the temperature profile inside the drop can be considered to be uniform and the energy balance on the drop is then given by

$$\rho_p C_p \frac{R_p}{3}\frac{dT}{dt} = -\frac{Q_a I}{4} - \left[\varphi_T k\left(\frac{\partial T}{\partial r}\right)_{r=R_p} + \varphi_M L D_g\left(\frac{\partial C}{\partial r}\right)_{r=R_p}\right] \qquad [8]$$

where Q_a and I are the particle absorption coefficient and the incident light intensity, respectively, k is the gas thermal conductivity, C_p is the drop heat capacity, L is the water latent heat of vaporization, and φ_T is the correction to the continuum Fourier heat flux to account for noncontinuum conditions. The correction above can be computed by assuming that the inside of the thermal boundary layer surrounding the drop heat transfer is described by Knudsen flow, while outside the boundary layer heat transfer follows the continuum conduction equation. By matching these two heat fluxes at the boundary layer the following expression can be obtained for φ_T (13):

$$\varphi_T = \frac{R_p}{R_p + l_T} \qquad [9]$$

where

$$l_T = \frac{k(2\pi MRT)^{1/2}}{\alpha_T P(C_v + R/2)} \qquad [10]$$

where α_T is the thermal accommodation coefficient, P and C_v are the gas pressure and heat capacity, respectively, and R is the gas constant.

Noting that the temperature and concentration fields in the gas phase are established much more quickly than the mass relaxation (1, 11) allows one to approximate the system as if in quasi-steady state. Equations [5] and [8] reduce to

$$\rho_p \frac{dR_p}{dt} = -\varphi_M D_g \frac{(C_s - C_\infty)}{R_p} \qquad [11]$$

and

$$\frac{Q_a I}{4} = \varphi_T k \frac{(T_s - T_\infty)}{R_p} + \varphi_M L D_g \frac{(C_s - C_\infty)}{R_p} \qquad [12]$$

where C_s and C_∞ are the vapor mass concentrations at the surface and far away from the drop, respectively.

Utilizing Raoult's Law and the Van't Hoff factor i to relate the vapor concentration over the surface of the salt solution to that of pure water gives

$$C_s = [1 - i(1 - X_w)]C^0 \qquad [13]$$

where X_w is the water mole fraction, and C^0 is the pure water concentration (on a mass basis).

The variation in water vapor concentration, C_s, with temperature is related to the temperature variation through the Clausius–Clapeyron equation:

$$\frac{dC^0}{C^0} = \left(\frac{LM}{RT} - 1\right)\frac{dT}{T}. \qquad [14]$$

By considering only small changes in the radius we let $R_p(t) = R_{p0} + \epsilon(t)$ where $\epsilon \ll R_{p0}$. Finally, substitution of Equations [12]–[14] into Equation [11] yields the following expression describing the growth rate of the particle:

$$\frac{d\epsilon}{dt} = -\alpha' I - \gamma' \epsilon \qquad [15]$$

where α' and γ' are

$$\alpha' = \left(\frac{Z}{1 + \frac{\varphi_M}{\varphi_T} LZ} \right) \frac{\varphi_M}{\varphi_T} \frac{Q_a}{4\rho_p} \qquad [16]$$

$$\gamma' = \frac{3D_g C^0 i X_w (1 - X_w)\varphi_M}{\rho_p R_{p0}^2 f_w \left(1 + \frac{\varphi_M}{\varphi_T} LZ\right)} + \frac{Q_a IZ}{4\rho_p \left(1 + \frac{\varphi_M}{\varphi_T} LZ\right)} \frac{\varphi_M}{\varphi_T} \qquad [17]$$

with

$$Z = \frac{D_g C^0}{kT} [1 - i(1 - X_w)] \left[\frac{LM}{RT} - 1 \right]. \qquad [18]$$

It should be noted that γ' reduces to that of Arnold *et al.* (1) in the continuum regime (i.e., for $\varphi_M = \varphi_T = 1.0$). Just as in that work, the second term in the equation for γ' may be neglected in comparison with the first term for the intensities used in this experiment.

At the low intensities used in the experiment the second term in Equation [17] (involving Q_a and I) is much smaller than the first term and can therefore be neglected. The relaxation rate of the particle radius is given by γ', and its inverse is the characteristic relaxation time τ of the particle. The ratio of the relaxation time to that in the continuum regime τ_c is obtained directly from Equation [17] as

$$\frac{\tau}{\tau_c} = \frac{1 + \frac{\varphi_M}{\varphi_T} LZ}{(1 + LZ)\varphi_M}. \qquad [19]$$

4. RESULTS AND DISCUSSION

The experimental relaxation times divided by the times predicted by the continuum theory are shown in Fig. 3. We also show the ratio of the theoretical noncontinuum relaxation time divided by the theoretical continuum time as expressed by Equation [19]. In the theoretical line both α_T and β_M were assumed to be unity. The proximity of the experimentally measured relaxation times and those predicted theoretically indicates that the experimental behavior matches the theoretical prediction quite well over the entire range under study. A summary of the conditions and the results of the experiments is shown in Table I. The differences in droplet composition seen in Table I are caused by small variations in the relative temperature of the chamber and the humidification bulb. It should be pointed out that we have attempted to obtain data at higher Knudsen numbers; however, at those conditions the scattered light signal became noisy due to oscillation of the droplet, therefore those data were not analyzed.

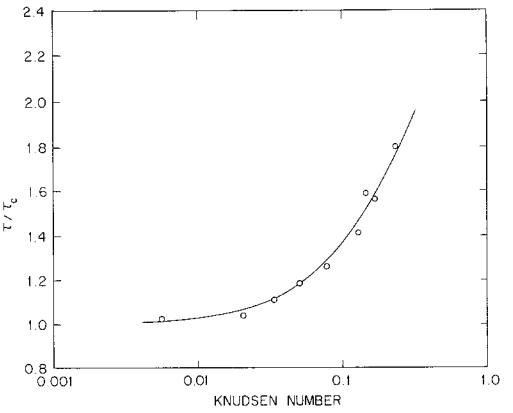

FIG. 3. Experimental relaxation times divided by the calculated theoretical time in the continuum regime, as a function of the Knudsen number. The solid line is the theoretically predicted ratio assuming α_T and $\beta_M = 1.0$.

To probe the sensitivity of these results to changes in the thermal accommodation and condensation coefficients, we first consider the value of the product (LZ) in the denominator of Equation [19]. Under the experimental conditions shown in Table I, Z ranged from 0.15 to 0.015 g/cal while L is on the order of 580 cal/g. Since both α_T and β_M appear to be of order unity in our case, the condition $(\varphi_M/$

TABLE I
A Summary of the Experimental Conditions during Various Runs

No.	Pressure (mm)	X_w	Temp. (°C)	Diameter (μm)	Kn	Relaxation time (ms)
1	21.6	0.91	23.70	13.6	0.239	600
2	34.9	0.91	24.31	12.6	0.172	280
3	43.7	0.89	25.01	11.8	0.150	230
4	51.4	0.88	25.92	11.7	0.132	155
5	48.8	0.92	23.85	19.3	0.079	930
6	79.9	0.92	23.85	19.3	0.052	900
7	121.5	0.91	24.06	18.8	0.035	610
8	203.9	0.90	24.25	18.8	0.021	575
9	736.1	0.90	23.25	19.3	0.0057	735

$\varphi_T)LZ \gg 1$ holds. Looking back at Equations [17] and [19], one immediately sees that, due to the large heat of condensation of water, the relaxation rate γ' is more or less independent of the noncontinuum correction factor φ_M. Since φ_M contains the water condensation coefficient β_M, the relaxation rate is therefore largely independent of the water condensation coefficient. Thus under these conditions $\tau/\tau_c \approx \varphi_T^{-1}$, and the ratio of the relaxation times equals the thermal noncontinuum correction factor.

In Fig. 4, we show the theoretical relaxation time divided by the continuum relaxation time as a function of Kn for a thermal accommodation coefficient $\alpha_T = 1.0$ and water vapor condensation coefficient of $\beta_M = 1.0$ and 0.1. The results in Fig. 4 indicate that it is not possible to determine conclusively the value of β_M from our data. The closeness of $\beta_M = 1.0$ and 0.1 curves was to be expected from our discussion above. In Fig. 5, we show the theoretical relaxation time divided by the continuum time as a function of Kn for a water vapor condensation coefficient $\beta_M = 1.0$ and thermal accommodation coefficient $\alpha_T = 1.0$, 0.8, and 0.5. As expected the relaxation time is more sensitive to the value of α_T than to the value of β_M. Moreover, the experimentally determined relaxation rates indicate that the value of the thermal accommodation coefficient is indeed close to unity.

In order to obtain a better estimate of the sticking coefficients for water in this system, the condition $(\varphi_M/\varphi_T)LZ \leqslant 1$ must hold. This condition can be achieved by repeating the

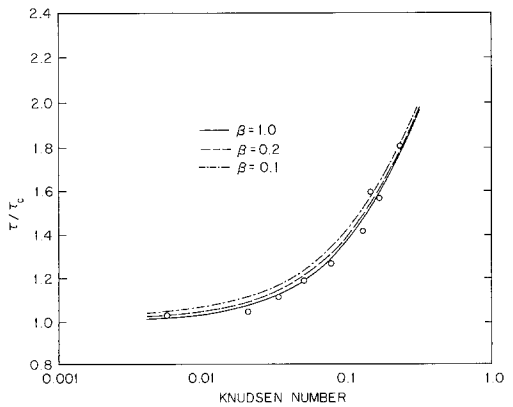

FIG. 4. The effect of the value of the mass condensation coefficient on the relaxation time, for $\alpha_T = 1.0$.

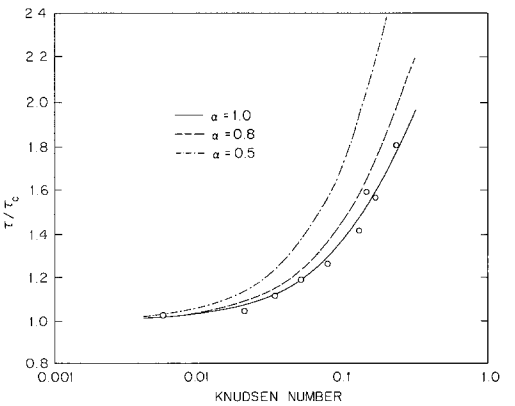

FIG. 5. The effect of the value of the thermal accommodation coefficient on the relaxation time, for $\beta_M = 1.0$.

experiments at a higher Knudsen number. Assuming that we work at a pressure of 25 Torr, a temperature of 25°C and a value of Z of about 0.05 g/cal implies that we need to achieve a Knudsen number of order 10.

5. CONCLUSIONS

We have reported the results of an experimental study of the growth of single aqueous solution droplets in the transition regime of heat and mass transfer. In the experiments $(NH_4)_2SO_4$ droplets of diameter between 10 and 20 μm were charged and levitated in an electrodynamic balance of quadrupole design, briefly heated from an IR radiation source to induce water evaporation, and then followed by light scattering as they relaxed back to their original equilibrium size. Knudsen numbers were varied between 0.23 and 0.0057 by controlling the total pressure in the system between 21.6 and 736.1 mm Hg.

The object of the experiments was twofold. First, it was desired to evaluate the extent of agreement between the measured relaxation times and those predicted by transition regime heat and mass transfer theories. Second, by comparison of the measured and predicted relaxation times in the transition regime, we wished to assess the ability to infer values of the thermal and mass accommodation coefficients, α_T and β_M, respectively, from such relaxation growth experiments.

We have found that the dependence of the measured relaxation times on Knudsen number is well represented by the available theories of heat and mass transfer in the continuum regime. Because of the large latent heat of vaporization of water, the growth process is controlled more by the heat transfer process than by mass transfer of water molecules to the drop. Consequently, it was not possible to infer a value of β_M from the data, although the data suggest that a value of β_M close to unity would not be an inconsistent interpretation. The data do afford a determination of α_T, and it was found that the data clearly support a value of $\alpha_T = 1$. This experimental determination supports the commonly made assumption that the thermal accommodation coefficient for aerosol particles is unity.

ACKNOWLEDGMENTS

This work was supported by U.S. Environmental Protection Agency Grant R-810857. S. Arnold was supported by a Chevron Visiting Professorship at the California Institute of Technology and by National Science Foundation Grant ATM-8413574. The authors thank Anthony B. Pluchino of the Aerospace Corporation and Thomas Dunn for their advice during this work.

REFERENCES

1. Arnold, S., Murphy, E. K., and Sageev, G., *Appl. Opt.* **24,** 1048 (1985).
2. Richardson, C. B., Lin, H. B., McGraw, R., and Tang, I. N., *Aerosol Sci. Tech.* **5,** 103 (1986).
3. Davis, E. J., *Aerosol Sci. Tech.* **2,** 121 (1983).
4. Davis, E. J., *Langmuir* **1,** 379 (1985).
5. Phillip, M. A., Gelbard, F., and Arnold, S., *J. Colloid Interface Sci.* **91,** 507 (1983).
6. Frickel, R. H., Shaffer, R. E., and Stamattoff, J. B., Technical report ARCSL-TR-77041. U.S. Army Armament Research and Development Command, Chemical Systems Laboratory, Aberdeen Proving Ground, Maryland, 1978.
7. Phillip, M. A., "An Absolute Method for Aerosol Particle Mass Measurement," p. 47. M.S. thesis, MIT, October 1981.
8. Arnold, S., *J. Aerosol Sci.* **10,** 49 (1979); Arnold, S., and Amani, Y., *Opt. Lett.* **5,** 242 (1980); Arnold, S., Amani, Y., and Orenstein, A., *Rev. Sci. Inst.* **51**(9), 1202 (1980).
9. Hamer, W. J., and Wu, Y. C., *J. Phys. Chem. Ref. Data* **1,** 1047 (1972).
10. Arnold, S., and Pluchino, A. B., *Appl. Opt.* **21,** 4194 (1982); Arnold, S., Newman, M., and Pluchino, A. B., *Opt. Soc. Amer.* **9,** 4 (1984).
11. Sageev, G., and Seinfeld, J. H., *Appl. Opt.* **23,** 4368 (1984).
12. Wagner, P. E., *in* "Particle Microphysics II" (W. H. Marlow, Ed.), pp. 129–178. Springer Verlag, Berlin.
13. Fukuta, N., and Walter, L. A., *J. Atmos. Sci.* **27,** 1160 (1970).
14. Armstrong, R. L., *Appl. Opt.* **23,** 148 (1984).
15. Sitarski, M., and Nowakowski, B., *J. Colloid Interface Sci.* **72,** 113 (1979).
16. Davis, E. J., and Ray, A. K., *J. Aerosol Sci.* **9,** 411 (1978).
17. Davis, E. J., Ravindran, P., and Ray, A. K., *Adv. Colloid Interface Sci.* **15,** 1 (1981).
18. Seinfeld, J. H., "Atmospheric Chemistry and Physics of Air Pollution." Wiley, New York, 1986.